



HAL
open science

Evaluation of Point Group Symmetry in Lanthanide(III) Complexes: A New Implementation of a Continuous Symmetry Operation Measure with Autonomous Assignment of the Principal Axis

Villads R. M. Nielsen, Boris Le Guennic, Thomas Just Sørensen

► **To cite this version:**

Villads R. M. Nielsen, Boris Le Guennic, Thomas Just Sørensen. Evaluation of Point Group Symmetry in Lanthanide(III) Complexes: A New Implementation of a Continuous Symmetry Operation Measure with Autonomous Assignment of the Principal Axis. *Journal of Physical Chemistry A*, 2024, 128 (28), pp.5740-5751. 10.1021/acs.jpca.4c00801 . hal-04646362

HAL Id: hal-04646362

<https://hal.science/hal-04646362v1>

Submitted on 9 Sep 2024

HAL is a multi-disciplinary open access archive for the deposit and dissemination of scientific research documents, whether they are published or not. The documents may come from teaching and research institutions in France or abroad, or from public or private research centers.

L'archive ouverte pluridisciplinaire **HAL**, est destinée au dépôt et à la diffusion de documents scientifiques de niveau recherche, publiés ou non, émanant des établissements d'enseignement et de recherche français ou étrangers, des laboratoires publics ou privés.



Distributed under a Creative Commons Attribution - NonCommercial 4.0 International License

Evaluation of Point Group Symmetry in Lanthanide(III) Complexes: A New Implementation of a Continuous Symmetry Operation Measure with Autonomous Assignment of the Principal Axis

Villads R. M. Nielsen¹, Boris Le Guennic² and Thomas Just Sørensen^{1}*

¹Department of Chemistry and NanoScience Centre, University of Copenhagen,
Universitetsparken 5, 2100 Copenhagen, Denmark

²Univ Rennes, CNRS, ISCR (Institut des Sciences Chimiques de Rennes), UMR 6226, 35000
Rennes, France

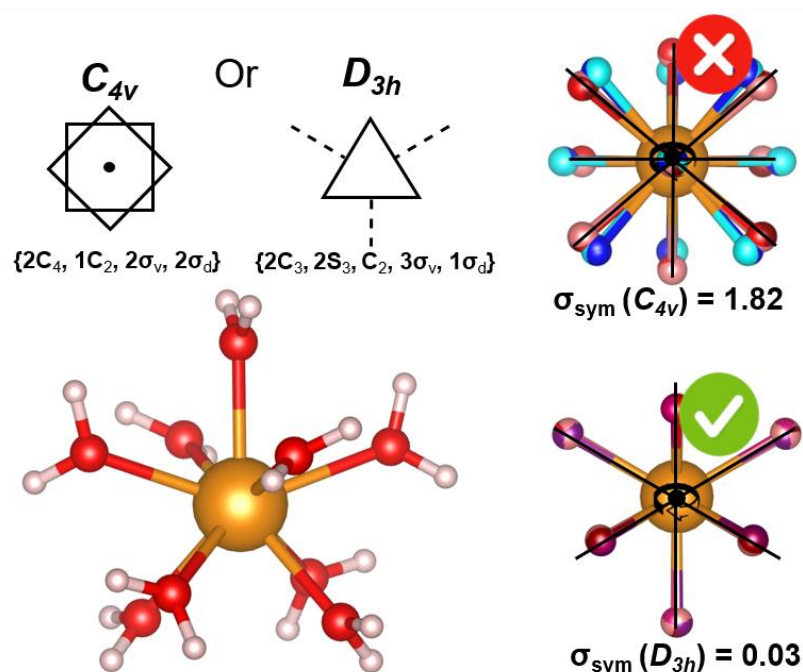
AUTHOR INFORMATION

*E-mail: tjs@chem.ku.dk

ABSTRACT: The structure of molecular systems dictates the physical properties, and symmetry is the determining factor for all electronic properties. This makes group theory a powerful tool in quantum mechanics to compute molecular properties. For inorganic compounds, the coordination geometry has been estimated as idealised polyhedra with high symmetry, which, through ligand field theory, provides predictive capabilities. However, real samples rarely have ideal symmetry, and although continuous shape measures (CShM) can be used to evaluate deviation from an ideal

reference structure σ_{ideal} , this often fails for lanthanide(III) complexes with high coordination numbers, no obvious choice of principal axes, and no obvious reference structure. In lanthanide complexes, the unique electronic structures and associated properties are intricately tied to the symmetry around the lanthanide center. Therefore, robust methodologies to evaluate and estimate point group symmetry are instrumental for building structure property relationships. Here, we have demonstrated an algorithmic approach that orients a molecular structure Q in the best possible way to the symmetry axis of any given point group G and computes a deviation from the ideal symmetry $\sigma_{\text{sym}}(G,Q)$. This approach does not compute the deviation from an ideal reference system, but the intrinsic deviation in the structure induced by symmetry operations. If the structure contains the symmetry operation, there is no deviation and $\sigma_{\text{sym}}(G,Q) = 0$. The σ_{sym} -deviation is generated from all the symmetry operation \hat{O}_S in a point group G using the most correct orientation of the sample structure in each group G . The best orientation is found by an algorithm that minimises the orientation of the structure with respect to G . To demonstrate the methodology, we have investigated the structure and symmetry of 8 and 9 coordinated lanthanide(III) aqua complexes and correlated the luminescence from 3 europium(III) crystals to their actual symmetry. To document the methodology, the approach has been tested on 26 molecules with different symmetry. It was concluded that the method is robust and fully autonomous.

TOC GRAPHICS



KEYWORDS Symmetry, Point Group, Coordination Chemistry, Lanthanide Luminescence.

Introduction

Two things determine the chemical and physical properties of a compound: constitution and conformation. In addition, further, the electronic properties of molecules, ions, and atoms are to a large extent determined by symmetry. The electronic structure can be simplified considering group theory,¹ and using crystal field (ligand field) theory, electronic transitions can be calculated.²⁻⁴ Symmetry dictates whether electronic transitions are allowed, which in turn enables the design of complexes with intricate photophysical properties.⁵⁻⁹ For the development of single-molecule magnets, tuning of symmetry plays an important role in both the magnetic behaviour and the relaxation pathways that can occur.¹⁰⁻¹⁴ As a final example, the charge flow in batteries is assumed to be controlled by defects, and understanding the deviations from ideal point group symmetry plays a crucial role in increasing the conductance in these.^{15, 16} So, in every field, from molecular

magnets to batteries, we need to be able to quantify the deviation from the ideal point group symmetry.

Symmetry is fundamentally a binary concept, either present or absent. Yet, in chemistry, experiments often indicate that approaching a given symmetry is enough for symmetry to be defining,^{1,2,4,7,8,13,17-19} thus defining symmetry as a continuous property is relevant. One approach is to define a measure of symmetry, that is, the distance the vertices of a structure has to change for the structure to contain a symmetry. This is the basis of the Continuous Symmetry Measure (CSM), first developed in 1992 by Zabrodsky, Peleg, and Avnir.²⁰ The CSM quantifies the symmetry of a structure Q as a continuous property. The CSM definition is general and does not calculate the distance to a selected reference structure. Instead, a structure P is defined to satisfy two criteria, it must be of the point group symmetry G evaluated with the CSM and it must have the minimal distance to Q, while still belonging to G. Typically, P is a polyhedron but can, in principle, be any structure as long as it has the same number of vertices as the evaluated structure Q.²¹ CSM defines a measure S(Q,G), which is the Euclidean distance between structure Q and the closest G-symmetric structure P. Specifically, S(Q,G) is the average distance between each vertex *k* of Q and P, the individual distances are given as $|Q_k - P_k|$. The obtained S(Q,G)-value is a normalized root mean square deviation defined as a value between 0 and 100, where 0 is perfect symmetry, see Eq. 1.

In order for CSM to provide the correct S(Q,G) value, only a single polyhedron P can be used, and this P has to be of a specific point group G. P is found by searching for the polyhedron that provides the shortest distance to Q, while being constrained to the symmetry G. Here, we adopt the definition of CSM by Peleg and Avnir shown in Eq. 1.

$$S(Q, G) = \min_P \sum_{k=1}^N \frac{|Q_k - P_k|^2}{|Q_k - Q_0|^2} \times \frac{100}{N} \text{ where } P|_G \text{ Equation 1.}$$

Where Q is a sample structure with k vertices, G is a point group symmetry, P is a structure with k vertices that is restricted to the symmetry G ($P|_G$) and has the minimal distance from Q, and N is the number of vertices k.

CSM has a practical problem: How to locate the specific P that satisfies Eq. 1. The 'folding-unfolding' method is in most implementations the solution applied to the problem. This algorithm renders P from Q based on a particular symmetry G.^{17, 20, 22} However, the methodology is cumbersome beyond the tetrahedron with four vertices ($k = 4$, coordination number 4, CN 4).^{17, 22}

A development on CSM is the Continuous Shape Measure (CShM). Instead of a minimising search for P, CShM directly compares a structure Q to a manually selected ideal reference structure P by calculating a deviation between the two, that is $\sigma_{ideal}(Q,P)$. The σ_{ideal} -value is the average distance between the vertices of structure Q and the reference P calculated in Eq. 2. This is mathematically the same Euclidean distance as calculated in Eq. 1. between the two structures (Q and P). The important difference is the expression of P. In CSM, the P is self-confined and must be generated from Q and G. In CShM, a manually selected reference structure is used, and the calculated quantity is the geometrical deviation $\sigma_{ideal}(Q,P)$ between the input structure Q and the ideal reference structure P.^{21, 23, 24} The definition of P and the transparency of the CShM implementation is critical, and different implementations have been published.^{17, 20-22, 25-38}

$$\sigma_{ideal}(Q, P) = \sum_{k=1}^N \frac{|Q_k - P_k|^2}{|Q_k - Q_0|^2} \times \frac{100}{N} \quad \text{Equation 2.}$$

The geometrical deviation $\sigma_{ideal}(Q,P)$ readily compares a structure to any polyhedron. CShM has been used to determine the deviation between various ideal polyhedra and metal complexes of CN 4,^{39, 40} CN 6,⁴¹ CN 7,⁴² CN 8,⁴³ CN 9,^{44, 45} and CN 10.⁴⁶ CShM provides physical information and has been used to quantify the distortions of coordination environments with temperature,⁴⁷⁻⁵⁰ and

to relate the physical properties of different metal oxides to different types of distortions of octahedral symmetry.^{51, 52}

CShM only accounts for symmetry indirectly, through the selected reference structures P. As symmetry determines molecular properties, we propose to directly quantify the distortion from symmetry. We propose that it be done by determining the deviation between the real structure Q and how it is reproduced as $\hat{O}_S Q$ by all the symmetry operations in the particular point group G. The Symmetry Operation Measure (SOM)⁵² is developed to quantify this deviation for an operation \hat{O}_S . SOM reports the deviation $\sigma_O(Q, \hat{O}_S Q)$ between structure Q and structure after it has been operated on by a symmetry operation. The deviation $\sigma_O(Q, \hat{O}_S Q)$ defined in Eq. 3 is mathematically identical to Eq. 2. and differ only in the reference used.

$$\sigma_O(Q, \hat{O}_S Q) = \sum_{k=1}^N \frac{|Q_k - \hat{O}_S Q_k|^2}{|Q_k - Q_0|^2} \times \frac{100}{N} \quad \text{Equation 3.}$$

SOM has been used to produce algorithms that classify molecular structures in terms of point group symmetry.⁵³⁻⁵⁷ The concept has been applied to reveal intricate trends in systems of both simple rotational symmetry,⁵⁸ of complex symmetry,^{59, 60} and further generalized to be applicable to vectors, functions, and operators within quantum mechanics.⁶¹⁻⁶³

In this study, we have implemented the mathematical framework of SOM to evaluate all the structural distortions needed to make a structure Q conform to a specific point group symmetry G. This is done by calculating the Euclidean distance from a structure to the structure after operated by each individual symmetry operation within a point group resulting in a total symmetry deviation from a specific point group: the $\sigma_{\text{sym}}(Q, G)$ -value. The implementation uses the SOM in Eq. 3. to calculate the Euclidean distance. We therefore propose the name Continuous Symmetry Operation Measure (CSOM), which demonstrates a resemblance to CSM and CShM, but employs the

mathematical framework of SOM. The main challenge of the CSoM approach is to align the molecular structure in the coordinate system (x',y',z') defined by the point group G in an autonomous way that is robust and transparent. For molecules that are distorted from perfect symmetry, the assignment of a principal axis can be ambiguous and is often not obvious. Furthermore, the methodology must be applicable to any molecular system and not just to a specific type of system.

Our implementation of CSoM is done in a program that identifies and minimizes the optimal orientation of any molecule of any composition Q, with respect to the primary symmetry axis of any point group G, by how well all symmetry operations \hat{O}_S of the point group reproduce the molecular structure. That is, we have made the CSoM generally applicable by autonomous identification of the correct principal symmetry axis using an approach that works for all point groups. To make the process fully transparent, the program outputs the deviations of both the overall symmetry $\sigma_{\text{sym}}(Q,G)$ and the deviation $\sigma_o(Q,\hat{O}_S Q)$ from each symmetry operation \hat{O}_S in each point group G investigated. The program also outputs all molecular structures $\hat{O}_S Q$ created by the symmetry operations for visual comparison. The program is implemented in Python and is made available as supporting information and from GitHub.

Methods

Computational details. Geometry optimizations of $[\text{Nd}(\text{H}_2\text{O})_q]^{3+}$ ($q = 8, 9$) were performed using density functional theory (DFT), with the hybrid meta-GGA M06-2X exchange correlation functional.⁶⁴ Calculations have been performed with the ADF suite (version 2022.103)⁶⁵ with basis sets at the TZP level for all atoms. The ZORA formalism with the MAPA potential was used

to describe scalar relativistic effects, and solvation of water was as implemented in ADF⁶⁶ using the COSMO model.⁶⁷

The input structures of $[\text{Nd}(\text{H}_2\text{O})_q]^{3+}$ ($q = 8, 9$) were constructed based on the model polyhedron structures provided in previous studies.^{68, 69} The mean Nd-O distance in each polyhedron was scaled to match the experimental results and set to 2.525 Å, as previously determined experimentally.⁷⁰ Hydrogen atoms were inserted manually and geometry optimized with fixed positions for Nd and O. From this, 8 input structures were constructed, four of CN = 8 and four of CN = 9. Furthermore, these structures were used as initial structures for complete geometry optimization with no fixed positions and were evaluated with a frequency analysis. The second sphere coordination structures were optimized with the geometry optimized CN = 8 and CN = 9 structures as initial geometries.

Geometry optimizations and frequency analysis were performed with the AMS 2023.1 program package (AMS 2023.1, SCM).⁷¹

Continuous Shape Measure CShM. CShM quantifies the difference between two geometrical structures with the same number of vertices. This is also called the geometrical deviation. The two geometrical structures, an input structure Q and an idealized polyhedron P, are aligned such that the total distance between the coordinates of all vertices between the two structures is minimised. This is performed with the Kabsch algorithm.⁷² The CShM value or $\sigma_{\text{ideal}}(\text{Q,P})$ value is the average distance between these two sets of coordinates describing Q and P normalized to the distance from the origin as formulated in Eq.2. We use just one implementation of the CShM formalism to calculate σ_{ideal} -Values.^{69, 73, 74}

Continuous Symmetry Operation Measure CSoM. CSoM quantifies how well a molecular structure Q is left unchanged by a specific symmetry operation \hat{O}_s or how well it is described by

a specific point group G . The structure Q is considered to have a point group G if all symmetry operations within a point group can be used on the structure to generate the same structure. The structure Q is considered to be distorted from a point group G if the symmetry operations produce a similar but distorted structure $Q' \neq Q$ instead of a structure identical to the original structure $\hat{O}_S Q = Q$. The distortion between a structure and the symmetry operated structure with respect to a specific symmetry operation is called σ_{sym} and is calculated with the SOM method as described in Eq. 3.

The quantification of how well a molecular structure Q belongs to a point group G and, therefore, how well the point group can be used to describe the structure, defined as $\sigma_{\text{sym}}(G, Q)$ that is the average distortion between the structure and the structure after all individual symmetry operations within the point group G . How σ_{sym} is calculated is described in Eq. 4. Using this formalism, all molecular structures can be evaluated and quantified as σ_{sym} -values for all point groups. All operations within a point group are applied to the coordinates of the molecular structure. The $\sigma_O(Q, \hat{O}_S Q)$ is calculated for the original structure Q which is evaluated against each structure created by a symmetry operation $\hat{O}_S Q$. This is defined in Eq. 3. When Q is operated with a symmetry operation, all coordinates and atom labels need to be compared to the original coordinates and atom labels. These two sets of labels are matched so that the total distance between the two sets of coordinates is minimal. This is done with the Hungarian algorithm⁷⁵, a solution to the permutation problem, implemented in Python with the Scipy module. The σ_{sym} -value is the sum of the $\sigma_O(Q, \hat{O}_S Q)$ -values normalised by the number of symmetry operations in the point group G .

The calculation of $\sigma_{\text{sym}}(Q, G)$ is implemented in a Python program that requires a molecular structure file with the atomic coordinates in .xyz format, and a list of point groups as input. The

program uses SciPy, NumPy, and Pandas. The program input is given as lists: ‘path_to_structures’ requires a list of the full path to each structure file in the .xyz format, and ‘point_group_names’ requires a list of point groups written in the format ‘pointgroup_G’.

The program includes all relevant point groups stored as .txt files (pointgroup_G.txt). For each point group (G) all symmetry operations \hat{O}_S are defined as a line with the \hat{O}_S name and 9 numbers representing the transformation matrix. When a point group is selected for analysis, the program reads each operation and constructs a 3x3 transformation matrix that is used as an operator on the input coordinate set. The resulting molecular structure is stored and used to calculate first $\sigma_O(Q, \hat{O}_S Q)$ and then $\sigma_{sym}(Q, G)$. The program handles atom labels and takes all sizes of structure with any combination of atoms. The program outputs $\sigma_{sym}(Q, G)$ for the selected G and all $\sigma_O(Q, \hat{O}_S Q)$, Q in the optimized Cartesian coordinate system (see below), and $Q' = \hat{O}_S Q$ for each G.

Note that all coordinates are normalised to 1 in Equation 1. and are effectively distortions quantified in terms of solid angle thus weighting absolute vector distortions closer to the origin more.

Orientation of the input structure. $\sigma_{sym}(Q, G)$ compares the structures to the symmetry operations of a point group G in a particular coordinate system, which should have the primary axis (z) in the molecular coordinate system as the main axis of symmetry. For the equation to provide the σ_{sym} -value, the molecular structure must be correctly oriented in this Cartesian coordinate system, that is, with the highest possible symmetry axis of the structure coinciding with the symmetry axis of the point group. This may be done by manual reorientation of the coordinates, but this may introduce errors resulting in a non-minimized σ_{sym} -value which will not provide the symmetry measure. Here, an algorithmic approach is used to automatically orient the input

structure to achieve the best possible match of the molecular axis (z) and the symmetry axis of a point group.

When the CSoM program runs the input coordinates $Q(x,y,z)$ against the point group list, the orientation of the molecular structure will be optimised for each point group G . For each G , 20 axes spanning half of the Fibonacci sphere are generated in the coordinate system (x,y,z) . Each of these axes defines a new Cartesian coordinate system (x',y',z') with a z' axis defined by a vector (a, b, c) . Each of the created z' axes has $\alpha = 0$, where α is the rotation angle of the $x'y'$ -plane perpendicular to z' . Rotational matrices are created to transform the input structure into these 20 Cartesian coordinate systems and $\sigma_{\text{sym}}(G,Q)$ are calculated. The $\sigma_{\text{sym}}(G,Q)$ is minimised by optimising the parameters a, b, c , and α that construct the coordinate system (x',y',z',α) using Powell's method as implemented in SciPy. After minimisation, the coordinate system with the lowest σ_{sym} -value is selected. The new coordinate system is expressed by defining the new z' axis as a vector (x', y', z') in the input coordinate system and a subsequent rotation angle (α) of the $x'y'$ plane. The optimized parameters (a,b,c,α) create a rotational matrix that is used to orient the input structure $Q(x,y,z,0)$ in the coordinate system $Q(x',y',z',\alpha)$ that gives the lowest $\sigma_{\text{sym}}(Q,G)$ for each selected G . Typically, multiple or even most of the 20 axes arrive at the same principle axis (z'), but since the $\sigma_{\text{sym}}(G,Q)$ -function contains many local minima, 20 axes are used to ensure that global minima are found every time. In our hands, 20 suffice, but more can be used at some computational expense.

The autonomous orientation of the coordinate system can be disabled and a manual coordinate system can be chosen with manual input for the principal axis (x,y,z) and the rotation angle (α) of the xy plane.

Results and Discussion

We are f-element chemists,⁷⁶ so let us consider a simple, yet often studied, model system: the lanthanide(III) aqua ion.^{70, 77} The molecular structures formed by this complex have either coordination number (CN) eight or nine. The molecular structure of these complexes is difficult to assess experimentally, and the structure is thought to be highly dynamic.⁶⁸ Using theory, the coordination geometry of monodentate ligands, such as water, is evaluated as the Thomson problem, which for CN = 8 and CN = 9 is solved to be of square antiprismatic geometry (SAP) and tricapped trigonal prismatic (TTP) geometry, respectively.^{78, 79} The SAP and TTP polyhedra are not the only low energy solutions, and four possible geometries are shown in Figure 1 for each coordination number. Table S1 contains an overview of the analysed polyhedra with the corresponding IUPAC nomenclature.⁸⁰ To investigate the possible molecular structures of lanthanide(III) aqua ions in water, we optimised the geometry of a neodymium(III) ion with density functional theory starting from the eight low energy solutions to the Thomson problem shown in Figure 1 (see computational details). The eight geometric optimisations converged to a single CN = 8 and a single CN = 9 structure only with minor geometrical differences. (See Figures S1-S2 and Tables S2-S3).

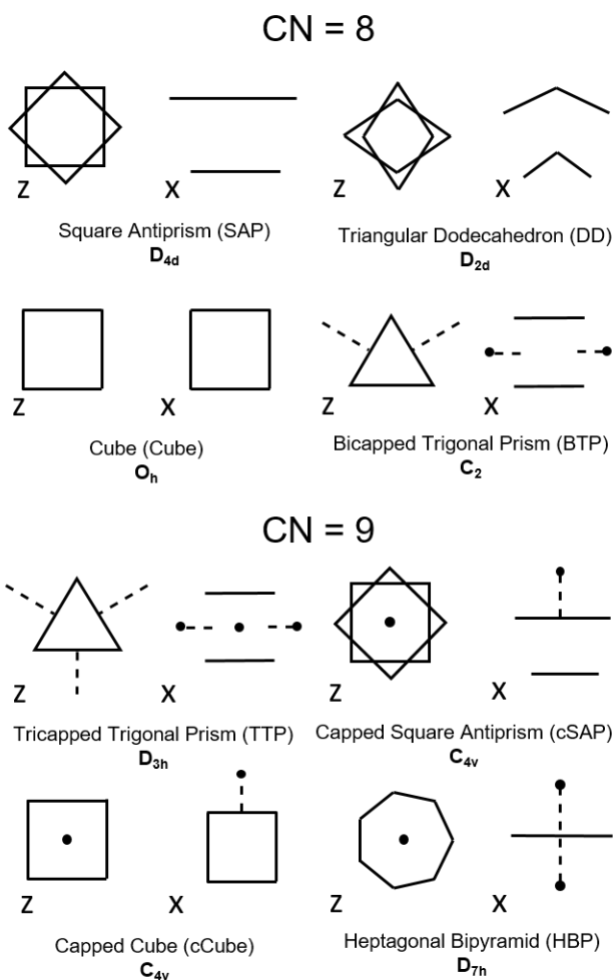


Figure 1. Eight idealized polyhedron that could describe 8- and 9-coordinated lanthanide(III) aqua complexes, four for coordination number 8 and four for coordination number 9.

Quantifying the shape of lanthanide(III) aqua complexes with CShM

To evaluate the geometry of our model systems, we applied the CShM methodology²¹ using the AlignIt approach⁶⁹ described in Eq. 2. Prior to this analysis, the two structures are aligned by a minimisation of the rotation matrix between the coordination structures. This is done for every possible permutation based on the Kabsch algorithm⁷² to ensure the most optimal overlap between the input structure Q and the reference structure P.

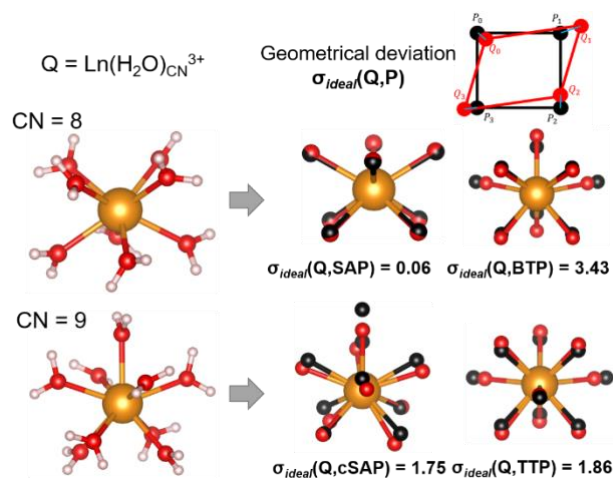


Figure 2. The two DFT optimized structures of 8- and 9-coordinated lanthanide(III) aqua complexes created from the four model polyhedra input structures. The optimised structures are shown with the optimised structural overlap with the SAP, DD (CN = 8) and cSAP, TTP (CN = 9) polyhedron of the model along with the deviation values, σ_{ideal} .

We investigated the eight constructed structures representing the molecular structure of the lanthanide(III) aqueous ion, four structures with [Ln(H₂O)₈]³⁺ and four structures of [Ln(H₂O)₉]³⁺. The geometrical distortions are calculated using Eq. 1. With the idealised polyhedra in Figure 1 as reference structures for the two molecular structures. These distortions are compiled in Table 1, along with all polyhedra evaluated against each other. The two polyhedra that best describe the structures are superimposed on the two optimised structures in Figure 2. We observe that although the SAP geometry near perfectly matches the [Ln(H₂O)₈]³⁺ structure, the TTP and cSAP are equally good descriptors for the [Ln(H₂O)₉]³⁺ structure. This poses a problem in the predictive power of the physical behaviour of the complex, as the symmetry, and therefore the electronic structure, of these geometries are different. Although we realise that this judgement is based on the selected ideal polyhedra used for comparison and a better version might exist, we conclude that CShM is not sufficient as a descriptor. The shapes for TTP and cSAP are not unique, and the

reference shapes used here may not be the closest representations of TTP and cSAP with respect to the $[\text{Ln}(\text{H}_2\text{O})_9]^{3+}$ structure. This introduces a significant selection bias in the CShM approach. To correctly identify the correct molecular structure of the 9-coordinated lanthanide(III) aqua complex, we could instead evaluate how well the structure is reproduced by the symmetry operations in the point groups of the evaluated polyhedra.

The Continuous Symmetry Operation Measure

The Continuous Symmetry Operation Measure (CSoM) is based on another geometric deviation value, σ_{O} , defined by SOM. However, rather than using a reference structure, the input structure Q is evaluated to itself after a symmetry operation $\hat{\text{O}}_s$ has been performed on the structure. The nomenclature of the deviation is changed from σ_{ideal} to σ_{O} to emphasise the difference. Averaging the deviation value calculated for each symmetry, excluding the identity operation, operation within a particular point group G gives the CSoM value $\sigma_{\text{sym}}(Q,G)$ defined in the equation. 4.

$$\sigma_{\text{sym}}(Q, G) = \sum_{s=1}^N \frac{\sigma_{\text{O}}(Q, \hat{\text{O}}_s Q)}{N} \quad \text{Equation 4.}$$

where $\sigma_{\text{O}}(Q, \hat{\text{O}}_s Q)$ is the geometry deviation defined in Equation 3 between the coordinate set of structure Q and the same coordinate set operated on by the specific symmetry operation $\hat{\text{O}}_s$. The sum is over all N symmetry operations in a point group, G . A visualisation of the σ_{sym} calculation is shown in Figure 3, where the different symmetry operations are applied to the calculated 9 coordinated lanthanide(III) aqua complex. Here, the complex has been evaluated in D_{3h} , C_{4v} , and D_{7h} symmetry using the optimal orientation with respect to the principle axis of each of the point groups. The visualisation readily identifies the correct symmetry as D_{3h} , since the atom positions are reproduced by the symmetry operation in D_{3h} and not in the other point groups. The computation of $\sigma_{\text{O}}(Q, \hat{\text{O}}_s Q)$ and σ_{sym} has been implemented in a Python program, which also

includes all point groups and symmetry operations. The program is available as supporting information.

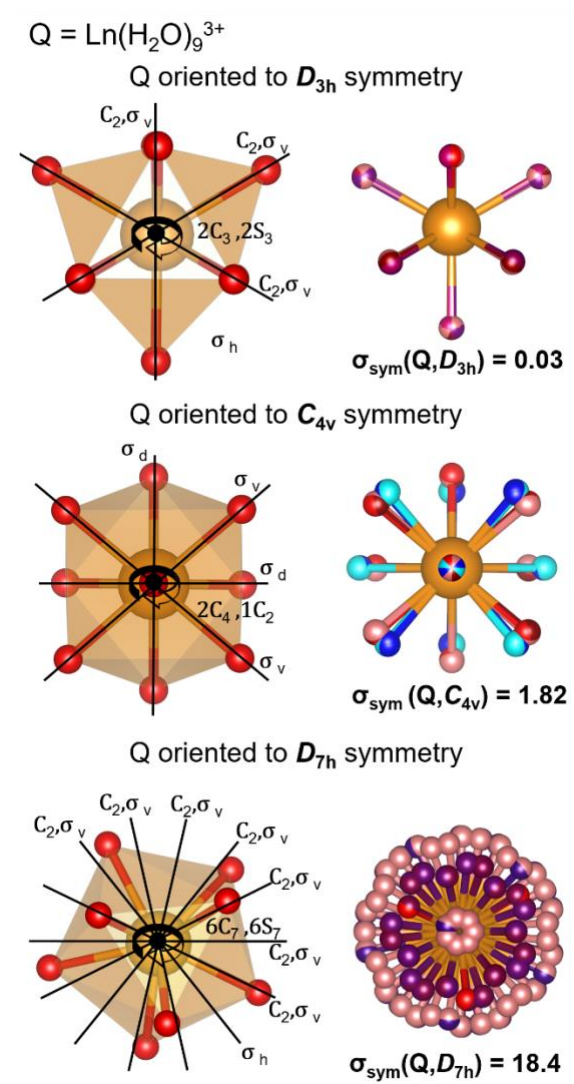
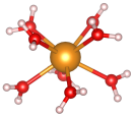
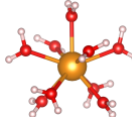

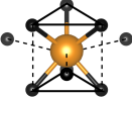
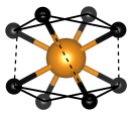

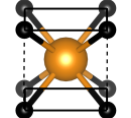
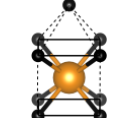
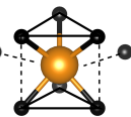
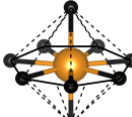


Figure 3. The DFT optimized structures (Q) of the 9-coordinated lanthanide(III) aqua complex analysed using three symmetries $G = D_{3h}$ (TTP, top), $G = C_{4v}$ (cSAP, middle) and $G = D_{7h}$ (HBP, bottom). The symmetry operations (\hat{O}_S) are shown on the input structure (Q). The algorithm outputs structures ($\hat{O}_S Q$) for each symmetry operation. These are plotted using different colors for the oxygen atoms for each output structure. If the symmetry is correct, the structures formed by symmetry operations on the input structure ($\hat{O}_S Q$) must overlap with the input structure (Q).

Table 1. Point group symmetry deviations, $\sigma_{\text{sym}}(\text{Q},\text{G})$, and CShM deviations calculated using AlignIT, $\sigma_{\text{ideal}}(\text{Q},\text{P})$, for the DFT-optimized structures (Q) and the ideal polyhedron structures (P).

| $\sigma_{\text{sym}}(\text{Q},\text{G})$ ($\sigma_{\text{ideal}}(\text{Q},\text{P})$) | $\text{G}=\text{D}_{4d}$ ($\text{P}=\text{SAP}$) | $\text{G}=\text{D}_{2d}$ ($\text{P}=\text{DD}$) | $\text{G}=\text{O}_h$ ($\text{P}=\text{Cube}$) | $\text{G}=\text{C}_{2v}$ ($\text{P}=\text{BTP}$) | $\sigma_{\text{sym}}(\text{Q},\text{G})$ ($\sigma_{\text{ideal}}(\text{Q},\text{P})$) | $\text{G}=\text{D}_{3h}$ ($\text{P}=\text{TTP}$) | $\text{G}=\text{C}_{4v}$ ($\text{P}=\text{cSAP}$) | $\text{G}=\text{C}_{4v}$ ($\text{P}=\text{cCube}$) | $\text{G}=\text{D}_{7h}$ ($\text{P}=\text{HBP}$) |
|--|---|--|---|---|---|---|--|---|---|
| CN = 8 optimised  | 0 (0.07) | 5.59 (2.92) | 19.00 (11.42) | 0 (3.43) | CN = 9 optimised  | 0.031 (1.86) | 1.818 (1.75) | 1.818 (12.26) | 18.424 (20.10) |
| SAP  | 0 (0) | 5.75 (2.55) | 19.39 (10.05) | 0 (4.54) | TTP  | 0 (0) | 4.28 (4.12) | 4.28 (13.24) | 22.103 (21.52) |
| DD  | 5.00 (2.55) | 0 (0) | 14.42 (7.21) | 0 (4.90) | cSAP  | 6.418 (4.13) | 0 (0) | 0 (9.08) | 22.85 (22.63) |
| Cube  | 14.06 (10.05) | 0 (7.21) | 0 (0) | 0 (14.41) | cCube  | 22.52 (12.87) | 0 (9.01) | 0 (0) | 20.46 (17.49) |
| BTP  | 6.233 (4.54) | 15.996 (4.82) | 28.709 (14.22) | 0 (0) | HBP  | 22.03 (21.35) | 18.66 (21.49) | 18.66 (15.87) | 0 (0) |

The autonomous solution to the problem of orienting the input structure in G

To calculate the true deviation from point group symmetry $\sigma_{\text{sym}}(\text{Q},\text{G})$, an optimal coordinate system must be found that aligns the molecular structure with the symmetry axis of each point group G. The symmetry axis, and thus the optimal coordinate system, is seldom obvious for lower

symmetry systems, where the choice of alignment can be ambiguous. Some algorithms solve this by detecting specific operations to decide on the point group through symmetry flow charts and manually chosen tolerance levels.^{53, 54} We propose that by optimising the coordinate system used to all symmetry operations of a given point group, a readily interpretable measure of the distortion from this point group can be obtained even when the point group is a poor descriptor. The algorithmic procedure is visualized in Figure 4a-b) for the ideal SAP polyhedron with the D_{4d} point group. The SAP polyhedron is point group D_{4d} and $\sigma_{\text{sym}}(\text{SAP}, D_{4d})$ must therefore be 0. With a randomly assigned coordinate system, the obtained value happens to be $\sigma_{\text{sym}} = 24.1$. To align the input structure, we numerically optimise σ_{sym} as a function of the coordinate system used, here defined by the direction of the principal z' axis in the input coordinate system (x, y, z) and the angle of rotation (α) of the $x'y'$ plane perpendicular to z' . The optimisation process is susceptible to the occurrence of local minima, as most structures exhibit some degree of symmetry from multiple points of view. In order to overcome this issue, we generate 20 evenly spaced vectors spanning half a Fibonacci sphere and use all 20 as trial coordinate systems. Numerically optimizing these provides multiple minima, but by clustering the results, it can be identified that three possible axes for the SAP structures are obtained with $\sigma_{\text{sym}} = 0$, $\sigma'_{\text{sym}} = 21.7$, and $\sigma''_{\text{sym}} = 23.4$ (see Figure S3-4 and Table S4 for details). Taking the coordinate system with the lowest σ_{sym} -value, we obtain the optimal orientation for the molecular structure in the coordinate system of the point group. We tested the method using 1 to 30 trial axes. Figure 4c shows the average symmetry deviation from 32 different point groups in four different polyhedra as a function of the number of trial axes. In our experiments, the optimal coordination system for the molecular structure tested was always found when 20+ trial axes were used (see Figure S5-7 for details). The approach described here is implemented in the Python scripts made available as SI

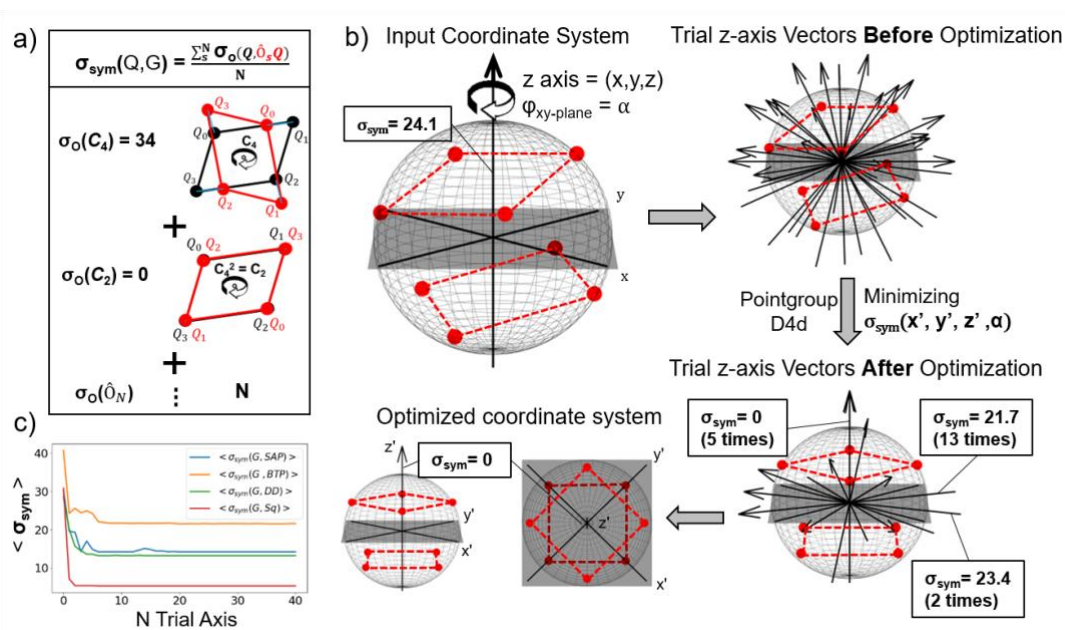


Figure 4. a) Visualisation of the calculation of σ_{sym} as the sum of distances from the original structure as a function of all symmetry operations in a point group. b) Visualisation of the optimization algorithm that finds the optimal coordinate system (x', y', z', α) as defined by a vector (x, y, z) in the input coordinate system and the rotation of the $x'y'$ -plane (α) for a molecular structure (Q) with respect to a selected point group (G). c) Convergence of the alignment algorithm displayed for the four CN = 8 polyhedra. The average symmetry deviation from all 32 different point groups is shown with respect to the number of trial z-axis used to determine the coordinate system for the molecular structure.

Quantifying the shape of lanthanide(III) aqua complexes with CSoM

Returning to the DFT optimised water complexes, and considering the idealized polyhedron from Figure 1, we are now ready to evaluate the distortion from point group symmetry of the computed molecular structures using CSoM. Table 1 shows the σ_{sym} -values, while the specific deviation from the individual operations of each point group is provided as SI (see Tables S5-S11). cursory inspection of Table 1 shows that the σ_{sym} values are 0 for the polyhedra that belong to the

point group. Note that if a point group results in a σ_{sym} -value of 0 then all groups that are subgroups to the evaluated point group must also give σ_{sym} -values of 0 eg, the C_{2v} point group, is a subgroup of the D_{4d} , D_{2d} , and O_h point groups, and 0 is obtained for C_{2v} .

The DFT optimised $[\text{Nd}(\text{H}_2\text{O})_8]^{3+}$ molecular structure is found to perfectly match the D_{4d} symmetry, which is expected from the near perfect geometrical match with SAP geometry. However, while the $[\text{Nd}(\text{H}_2\text{O})_9]^{3+}$ molecular structure was found to be directly between the reference TTP and cSAP geometries using CShM, the CSM analysis shows that the $[\text{Nd}(\text{H}_2\text{O})_9]^{3+}$ molecular structure matches the D_{3h} symmetry, see Table 1 and Figure 3, which includes the visualization of the CSoM calculation using the D_{3h} , C_{4v} , and D_{7h} point groups. Note that the optimal coordinate system of the molecular structure Q is different for all three point groups G . The contribution of individual symmetry operations to $\sigma_{\text{sym}}(G, Q)$ is also calculated (see Tables S5-S11), and while all operations within D_{3h} are approaching $\sigma_{\text{sym}} = 0$, all operations within D_{7h} give very large σ_{sym} -values indicating no presence of D_{7h} symmetry.

The structure is therefore best described by the TTP geometry, but not by the reference TTP geometry used; see above. We thus conclude that the $[\text{Nd}(\text{H}_2\text{O})_9]^{3+}$ molecular structure has almost perfect D_{3h} symmetry, despite the poor match to the reference TTP geometry used in Figure 2. With D_{3h} symmetry the structure must be assigned to TTP geometry, but one with slightly different angles and ratios of bond lengths between the capping and trigonal oxygen than those found in the ideal reference polyhedra. Despite the differences, the structure is within the D_{3h} point group. Visualisation in Figure 3 allows the same conclusion to be drawn without scrutiny of the numbers.

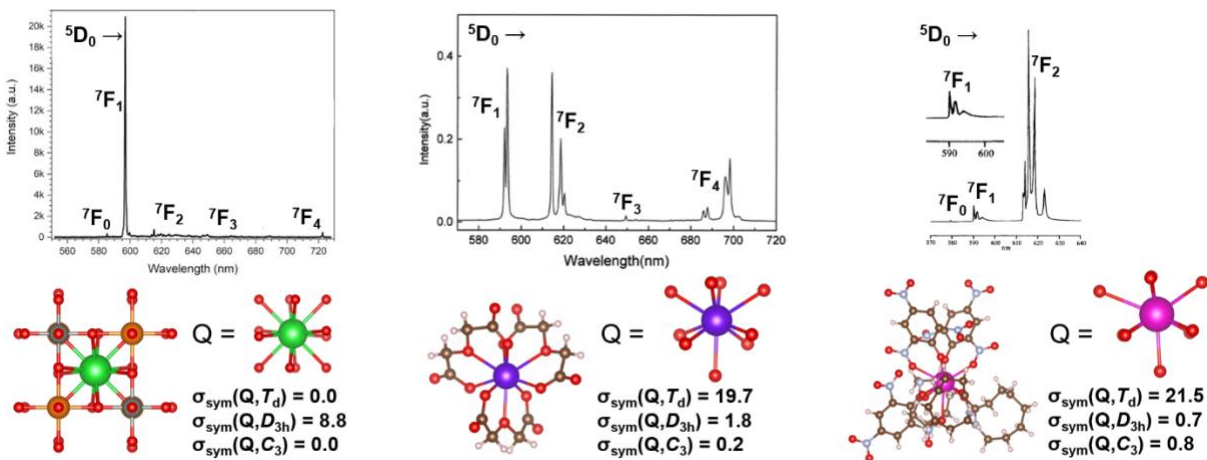


Figure 5. Spectra, structure and determined CSoM values ($\sigma_{\text{sym}}(\text{Q}, \text{G})$) for three europium(III) structures. Left: Europium(III)-doped Ba_2MgWO_6 double perovskite, redrawn with permission from reference 81. Copyright 2019, Elsevier. The structure is shown with the symmetry optimized C_4 perpendicular to the plane. Middle: $\text{Eu}(\text{ODA})_3$, redrawn with permission from reference 82. Available under a CC-BY NC license. Copyright J.-G. Kang. The structure is shown with the symmetry optimized C_3 perpendicular to the plane. Right: $\text{Eu}(\text{pic})_3 \cdot 3(\text{aza})$, redrawn with permission from reference 83. Copyright 1997, Elsevier. The structure is shown with the symmetry optimized C_3 perpendicular to the plane.

Example usage for rationalising europium(III) luminescence

Moving beyond our model system, three europium(III) structures from the literature were investigated. Europium(III) is commonly used to probe point group symmetry in a coordination complex as the emission spectra are relatively easily interpreted.⁸⁴⁻⁸⁷ This is due to the singly degenerate nature of the emitting state, 5D_0 , and the concise empirical rules that relate to the splitting of the 7F_J states.⁸⁸ Thus, the emission spectra of europium(III) can be used to evaluate the symmetry of the complex. The transitions of $^5D_0 \rightarrow ^7F_0$, 7F_1 , and 7F_2 is of special interest and a small recap of the analysis procedure is given here:⁸⁸

- The ${}^5D_0 \rightarrow {}^7F_0$ line contains up to one line. If a mirror plane vertical to the principal axis is present, the transition probability of this transition vanishes, and no transition will be observed.
- The ${}^5D_0 \rightarrow {}^7F_1$ band contains up to three lines. If the system is tetragonal or hexagonal, e.g., if C_3 or C_4 symmetry is present, two of the states in 7F_1 will be degenerate. If the system is cubic, all three states in 7F_1 will be degenerate. Spectroscopically, this results in only two or one transition to be observed instead of three, respectively.
- The ${}^5D_0 \rightarrow {}^7F_2$ band contains up to five lines. If the system is tetragonal, four states can be observed, which is further reduced to three for trigonal and hexagonal and two for cubic symmetry.

Figure 5 shows the spectra and molecular structures of three different europium(III) complexes from the literature: an Eu(III) doped Ba_2MgWO_6 double perovskite,⁸¹ $Eu(ODA)_3$,⁸² and $Eu(pic)_3 \cdot 3(aza)$.⁸³ The point group symmetry of europium(III) in these crystals are reported to be O_h , D_{3h} , and C_{3v} respectively. We re-evaluated these point group assignments using our implementation of the CSoM methodology. Taking into account only the inner sphere oxygen atom - shown isolated in Figure 5 - we have CN = 12, CN = 9, and CN = 9 molecular structures. The σ_{sym} -values are provided for 26 different point groups in the SI (see Table S13) and for T_d , D_{3h} and C_3 in Figure 5. We find that none of the three original point group assignments matches the structures. For $Eu:Ba_2MgWO_6$ we find that the distortion from O_h was $\sigma_{sym} = 0.6$, which is a low value and the structure is close to O_h , but T_d is a perfect match with $\sigma_{sym} = 0.0$. In the emission spectrum, only a single peak is observed for the ${}^5D_0 \rightarrow {}^7F_1$ transition as is expected from both T_d and O_h symmetry. The $Eu(ODA)_3$ system can, with a $\sigma_{sym} = 1.3$, be described as a heavily distorted D_{3h} system, but it is significantly better described as C_3 with $\sigma_{sym} = 0.2$. In the emission spectra

two peaks in 7F_1 and three in 7F_2 are observed, which is the expected lines with either of the two point groups. $\text{Eu}(\text{pic})_3 \cdot 3(\text{aza})$ can be described as heavily distorted from the point groups, D_{3h} , C_{3v} , or C_3 with $\sigma_{\text{sym}} = 0.7, 0.8,$ and 0.8 respectively. Consulting the emission spectra, three lines are observed in ${}^5D_0 \rightarrow {}^7F_1$ and five lines in ${}^5D_0 \rightarrow {}^7F_2$ indicating that this degree of distortion is enough to completely distort the physical symmetry of the electronic structure, resulting in the interpretation of C_1 symmetry.

Table 2. σ_{sym} -values calculated for 26 molecules (Q) sorted by their point group symmetry are evaluated with 26 different point groups (G). Green elements highlight the assigned point group, and orange elements highlight the subgroups of the assigned point group.

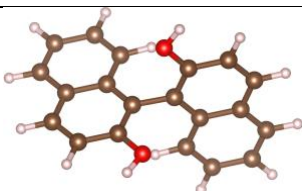
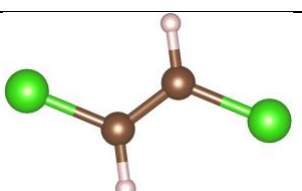
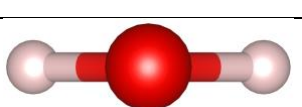
| Q | G | | | | | | | | | | | | | | | | | | | | | | | | | | | |
|--|----------------|----------------|----------------|-----------------|-----------------|----------------|-----------------|-----------------|-----------------|-----------------|----------------|----------------|-----------------|-----------------|----------------|-----------------|-----------------|-----------------|-----------------|-----------------|-----------------|-----------------|----------------|----------------|----------------|----------------|--|--|
| | C _i | C _s | C ₂ | C _{2h} | C _{2v} | C ₃ | C _{3h} | C _{3v} | C _{4v} | C _{5v} | S ₄ | D ₂ | D _{2d} | D _{2h} | D ₃ | D _{3d} | D _{3h} | D _{4d} | D _{4h} | D _{5d} | D _{5h} | D _{6h} | T _d | T _h | O _h | I _h | | |
| CH ₂ Cl ₂ F ₂ | 0 | 23.4 | 23.4 | 15.6 | 37.2 | 91.7 | 69.2 | 61.1 | 68 | 64.2 | 83.7 | 37.2 | 68 | 31.9 | 71.7 | 65.2 | 62.5 | 60.6 | 62.7 | 57 | 62.5 | 52.1 | 104 | 99.6 | 102 | 95.9 | | |
| CH ₂ ClF | 219 | 0 | 102 | 146 | 68.1 | 100 | 132 | 74.5 | 79.6 | 75.1 | 146 | 125 | 125 | 132 | 120 | 109 | 116 | 117 | 126 | 115 | 104 | 138 | 137 | 135 | 133 | | | |
| C ₂₀ H ₁₄ O ₂ | 82.5 | 21.3 | 0 | 54 | 26.2 | 62.3 | 50.6 | 51.4 | 50.9 | 47.9 | 28.7 | 25.8 | 24.6 | 47.7 | 49.5 | 46.2 | 43 | 42.8 | 49.4 | 47.4 | 45.8 | 38.4 | 64.1 | 74.7 | 71.9 | 75.5 | | |
| C ₂ F ₂ H ₂ | 0 | 0 | 0 | 0 | 30.2 | 67.4 | 51.3 | 48.7 | 50.6 | 47 | 62.8 | 30.2 | 50.6 | 25.9 | 53.9 | 49 | 46.4 | 41.9 | 46.1 | 41.6 | 46.2 | 38.8 | 103 | 99 | 100 | 96.6 | | |
| H ₂ O | 126 | 0 | 0 | 84.1 | 0 | 63.2 | 75.8 | 63.2 | 57.2 | 49.5 | 84.2 | 84.2 | 72.1 | 72.1 | 75.8 | 68.9 | 57.4 | 55.4 | 63.1 | 72.5 | 66.5 | 60.1 | 130 | 127 | 127 | 122 | | |
| MC ₁₈ H ₁₅ | 86.1 | 11.2 | 45.5 | 61.2 | 28.8 | 0 | 41.6 | 5.61 | 27.1 | 24.7 | 72.1 | 65.7 | 59.1 | 56.1 | 32.1 | 47.5 | 41.9 | 49.8 | 57.2 | 53.1 | 53.1 | 52.5 | 78.8 | 83.8 | 80.3 | 88.4 | | |
| BO ₃ H ₃ | 85.7 | 0 | 3.41 | 45.9 | 2.27 | 0 | 0 | 1.7 | 35 | 31.8 | 43.9 | 45.9 | 35 | 39.3 | 2.04 | 37.5 | 1.55 | 26.2 | 30.8 | 34.1 | 30.1 | 31.1 | 46.1 | 66.4 | 65.8 | 63.3 | | |
| NH ₃ | 112 | 0 | 37.2 | 62.9 | 24.8 | 0 | 22.3 | 0 | 30.2 | 27.6 | 62.9 | 62.9 | 51.5 | 53.9 | 22.3 | 51.4 | 23.6 | 42.4 | 47.9 | 49.2 | 45.7 | 46.8 | 58.2 | 76.1 | 75.2 | 73.8 | | |
| MF ₅ Cl | 114 | 0 | 0 | 72.2 | 0 | 15.3 | 53.7 | 9.59 | 0 | 12.2 | 68.7 | 68.7 | 61.4 | 61.9 | 53.7 | 63.5 | 42.6 | 52.5 | 60.7 | 64.8 | 60 | 54.3 | 60.7 | 60.7 | 59.4 | 69.9 | | |
| MF ₆ Cl | 124 | 0 | 23.9 | 75.5 | 12 | 10.8 | 61.3 | 6.77 | 9.49 | 0 | 68.1 | 68 | 58 | 63.9 | 62.7 | 59.9 | 51 | 55 | 60.8 | 59.2 | 50.7 | 58 | 58 | 65.4 | 64.4 | 63.3 | | |
| C ₂₅ H ₂₀ | 46.9 | 0.002 | 0 | 29.8 | 0.001 | 15.9 | 27.5 | 11.9 | 25.2 | 26.3 | 0 | 0.001 | 0.001 | 25.6 | 22 | 28.1 | 22.2 | 27.4 | 22.7 | 27.5 | 26.6 | 22.9 | 22.2 | 26.9 | 26.5 | 36.8 | | |
| C ₂ H ₄ (α = 10°) | 2.96 | 2.96 | 0 | 1.97 | 1.97 | 24.5 | 20.8 | 25.3 | 24.1 | 19.2 | 21.5 | 0 | 18 | 1.69 | 19.6 | 18.9 | 18.9 | 19.5 | 19.5 | 18.3 | 18.8 | 15.2 | 74.1 | 72.4 | 74.7 | 76.2 | | |
| C ₂ H ₄ (α = 90°) | 49 | 0 | 0 | 25.9 | 0 | 24.5 | 22.3 | 15.5 | 22.2 | 19.2 | 0 | 0 | 0 | 22.2 | 19.6 | 19.6 | 20.2 | 19.4 | 21 | 20.3 | 18.8 | 15.9 | 55.8 | 76.6 | 75.1 | 73.8 | | |
| C ₂ H ₄ (α = 0°) | 0 | 0 | 0 | 0 | 0 | 24.5 | 19.6 | 24.5 | 22.2 | 19.2 | 32.7 | 0 | 22.2 | 0 | 19.6 | 17.8 | 17.8 | 19.4 | 21 | 17.7 | 18.2 | 14 | 75.1 | 71 | 73.5 | 76 | | |
| MC ₆ H ₂₄ N ₆ Cl ₂ | 14.4 | 14.4 | 0 | 9.6 | 12.7 | 0 | 11.4 | 7.2 | 20 | 19.1 | 24 | 17.3 | 19.8 | 16.2 | 0 | 7.85 | 10.4 | 15.8 | 18.6 | 18 | 18.2 | 15.6 | 23.2 | 23.2 | 22.7 | 30.1 | | |
| C ₂ H ₆ (α = 90°) | 0 | 0 | 0 | 0 | 17 | 0 | 19.9 | 0 | 13.6 | 12.4 | 17.1 | 17.1 | 13.6 | 14.6 | 0 | 0 | 16 | 10.1 | 12 | 11.4 | 12.2 | 11.5 | 33.9 | 33.9 | 33.1 | 54.6 | | |
| C ₂ H ₆ (α = 0°) | 33.3 | 0 | 0 | 17 | 0 | 0 | 0 | 0 | 13.6 | 12.4 | 17.1 | 17.1 | 13.6 | 14.6 | 0 | 13.9 | 0 | 10.1 | 12 | 13.3 | 11.7 | 11.5 | 53.8 | 56.8 | 54 | 56.5 | | |
| S ₈ | 18.3 | 0 | 0 | 12.2 | 0 | 24.8 | 16.2 | 15.7 | 0 | 13.4 | 12.2 | 12.2 | 10.5 | 10.5 | 16.2 | 13.9 | 13.8 | 0 | 9.19 | 14 | 13.1 | 9.87 | 47.9 | 47.8 | 46.9 | 48.3 | | |
| MCl ₄ | 0 | 0 | 0 | 0 | 0 | 21.4 | 17.2 | 13.4 | 0 | 17.1 | 0 | 0 | 0 | 0 | 17.2 | 15.6 | 13.2 | 19 | 0 | 14.6 | 16.2 | 12.3 | 45.6 | 42.2 | 44.6 | 49.3 | | |
| MO ₁₀ (α = 90°) | 0 | 0 | 0 | 0 | 7.32 | 11.8 | 11.1 | 7.39 | 11.3 | 0 | 13.2 | 7.32 | 11.3 | 6.27 | 9.43 | 8.58 | 10.1 | 7.7 | 10.5 | 0 | 10.4 | 8.78 | 16.3 | 14.8 | 15.9 | 14.4 | | |
| MH ₁₀ (α = 0°) | 21.3 | 0 | 0 | 10.7 | 0 | 9.65 | 7.72 | 9.65 | 8.48 | 0 | 10.7 | 10.7 | 8.48 | 9.21 | 7.72 | 7.96 | 5.96 | 6.3 | 7.48 | 8.48 | 0 | 7.19 | 18.4 | 18.8 | 18.4 | 23.9 | | |
| C ₆ H ₆ | 0 | 0 | 0 | 0 | 0 | 0 | 0 | 0 | 11.6 | 9.62 | 17.9 | 0 | 11.6 | 0 | 0 | 0 | 0 | 9.91 | 11 | 8.21 | 9.12 | 0 | 52.2 | 50.2 | 51.1 | 49.9 | | |
| CH ₄ | 106 | 0 | 0 | 56.3 | 0 | 0 | 30.4 | 0 | 21.7 | 19.8 | 0 | 0 | 0 | 45.6 | 33.4 | 42.7 | 28.8 | 39.4 | 40.7 | 44.2 | 39.7 | 34.2 | 0 | 42.3 | 41.6 | 42.5 | | |
| C ₆₀ Br ₂₄ | 0 | 0 | 0 | 0 | 0 | 0 | 3.18 | 1.61 | 0.98 | 3.11 | 1.15 | 0 | 0.98 | 0 | 1.03 | 0.94 | 4.02 | 2.9 | 0.86 | 2.76 | 4.67 | 3.58 | 0.90 | 0 | 0.88 | 2.7 | | |
| MF ₆ | 0 | 0 | 0 | 0 | 0 | 0 | 12.3 | 0 | 0 | 12.2 | 0 | 0 | 0 | 0 | 0 | 0 | 9.46 | 13.6 | 0 | 10.4 | 11.5 | 8.75 | 0 | 0 | 0 | 25.3 | | |
| C ₆₀ | 0 | 0 | 0 | 0 | 0 | 0 | 2.54 | 0 | 1.41 | 0 | 1.64 | 0 | 1.41 | 0 | 0 | 0 | 2.34 | 3.07 | 1.23 | 0 | 3.01 | 2.02 | 1.29 | 0 | 1.26 | 0 | | |


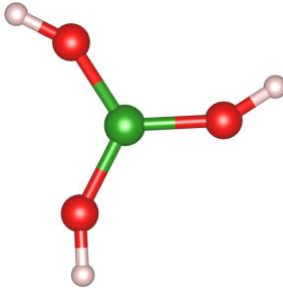
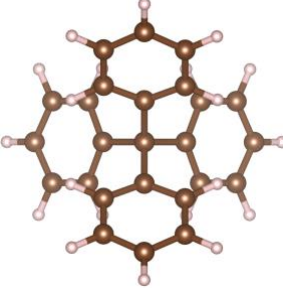
The Implementation of CSoM as a General Tool for Symmetry Quantification

To show that the method is generally applicable, we evaluated 26 molecules of different symmetry (see Figure S8 for visualisation of the structures). The results compiled in Table 2 show that the method is robust, and both the algorithm to find the primary axis and our implementation

of CSoM is generally applicable. To illustrate how the method reports the values of the individual symmetry operations, we included these values from six systems in Table 3. Scrutiny of Table 3 shows how the method handles each of the symmetry operations and it is easily recognised how a symmetry element present in a molecular structure is clearly recognised with a low number and how a symmetry element not present results in a high number.

Table 3. Individual symmetry operations of molecules of specific point group symmetries. Values are with respect to the optimised principal axis of highest symmetry. Values in parentheses are with the principle axis optimised to the individual symmetry operation.

| Q Formula (G) | $\sigma_o(Q, \hat{O}_s Q)$ | | | | | | | |
|--|----------------------------|-------|----------------|----------------|----------|----------------|----------------|-----------------|
| | \hat{O}_s | | | | | | | |
| | E | i | $\sigma_h(z)$ | $\sigma_v(y)$ | $C_2(z)$ | $C_3(z)$ | $C_3^2(z)$ | $S_4(z)$ |
|  $C_{20}H_{14}O_2$ (C_2) | 0 | 82.5 | 82.5 (21.3) | 63.3 (21.3) | 0 | 82.0 (62.2) | 65.8 (62.2) | 116.9 (23.6) |
|  $C_2F_2H_2$ (C_{2h}) | 0 | 0 | 0 | 61.5 (0) | 0 | 100 (67.4) | 100 (67.4) | 200 (57.1) |
|  H_2O (C_{2v}) | 0 | 126.3 | 126.3 (0) | 0 | 0 | 63.2 (63.2) | 63.2 (63.2) | 252.6 (63.1) |

| | | | | | | | | |
|---|---|-------|----------------|----------------|----------------|----------------|----------------|----------------|
|  $\text{PC}_{18}\text{H}_{15}$ (C_3) | 0 | 100.6 | 69.4 (11.2) | 25.4 (11.2) | 45.7 (50.0) | 0 | 0 | 97.6 (73.2) |
|  BO_3H_3 (C_{3h}) | 0 | 85.7 | 0 | 15.2 (0) | 85.7 (3.4) | 0 | 0 | 23.0 (23.0) |
|  $\text{C}_{25}\text{H}_{20}$ (S_4) | 0 | 46.9 | 46.9 (0) | 0 (0) | 0 | 36.9 (15.9) | 36.7 (15.9) | 0 |

Conclusions

We have reported an implementation of the continuous symmetry operation measure CSOM; an alternative to quantify symmetry deviations with the continuous symmetry measure. The implementation evaluates how well a molecular structure contains the symmetry of an entire point group. This is achieved by aligning a molecular structure Q in the optimal coordinate system for a given point group symmetry G , and then calculating a deviation from this symmetry $\sigma_{\text{sym}}(G, Q)$.

The deviation calculates the overlap between the structure and itself after being operated by each individual symmetry operation in the group. In the examination of 8- and 9-coordinated lanthanide(III) aqua complexes, we found that while the continuous shape measure was insufficient to describe the symmetry of the 9-coordinated complexes, the continuous symmetry operation measure reported here provided an accurate evaluation of the symmetry point group. We conclude that the combination of both measures is useful to provide a comprehensive picture of the coordination structure.

We have documented robust performance on a large series of molecules, and used the new CSoM methodology on lanthanide(III) complexes with 8, 9 and 12 donor atoms in the inner coordination sphere. The method was developed by expanding on previously reported approaches,^{17, 89} and adding a minimisation algorithm to search for the optimal coordinate system for each tested symmetry.

Testing the methodology to three europium(III) complexes from the literature, we showed that we could reevaluate the point group symmetry assignment of the structures, and we could relate the CSoM identified point groups to the observed electronic transitions in the emission spectra. With the CSoM method reported here, we can readily evaluate point group symmetry through a robust methodology made available as Python code.

ASSOCIATED CONTENT

The following files are available free of charge. Supporting information (PDF), details on the geometry optimizations, the optimizations of the principal axis, documentation of convergence, and extended details on the symmetry deviations calculations.

Structure files (.xyz), coordinates of all structures discussed.

Python script (.py), the symmetry deviation program written in Python.

Corresponding Author

* Department of Chemistry & Nano-Science Center, University of Copenhagen, Universitetsparken 5, DK2100 Kbenhavn, Denmark, tjs@chem.ku.dk

ACKNOWLEDGMENT

The authors thank the Carlsberg Foundation, Villum Fonden, Novo Nordisk Fonden, Independent Research Fund Denmark, Tranes Foundation, William Demand Foundation and the University of Copenhagen for generous support.

Funding Sources

The Carlsberg Foundation, Villum Fonden, Novo Nordisk Fonden, Independent Research Fund Denmark, Tranes Foundation, and the William Demand Foundation.

References

- (1) Cioslowski, J.; Strasburger, K. Symmetry Equiincidence of Natural Orbitals. *The Journal of Physical Chemistry Letters* **2023**, *14* (41), 9296-9303.
- (2) Heit, Y. N.; Gendron, F.; Autschbach, J. Calculation of Dipole-Forbidden 5f Absorption Spectra of Uranium(V) Hexa-Halide Complexes. *The Journal of Physical Chemistry Letters* **2018**, *9* (4), 887-894.
- (3) Sinha, N.; Wenger, O. S. Photoactive Metal-to-Ligand Charge Transfer Excited States in 3d6 Complexes with Cr0, Mni, Feii, and Coiii. *Journal of the American Chemical Society* **2023**, *145* (9), 4903-4920.

- (4) Kazmierczak, N. P.; Mirzoyan, R.; Hadt, R. G. The Impact of Ligand Field Symmetry on Molecular Qubit Coherence. *Journal of the American Chemical Society* **2021**, *143* (42), 17305-17315.
- (5) Lyu, Z.-Y.; Dong, H.; Yang, X.-F.; Sun, L.-D.; Yan, C.-H. Highly Polarized Upconversion Emissions from Lanthanide-Doped LiYF₄ Crystals as Spatial Orientation Indicators. *The Journal of Physical Chemistry Letters* **2021**, *12* (46), 11288-11294.
- (6) Chen, X.; Ge, L.; Tang, Y.; Han, C.; Yu, Y.; Liu, S.; Li, M.; Zhang, P.; Xu, L.; Yin, J.; et al. Achieving Ultralong Room-Temperature Phosphorescence in Two-Dimensional Metal Halide Perovskites by Alkyl Chain Engineering. *The Journal of Physical Chemistry Letters* **2023**, *14* (38), 8638-8647.
- (7) Zhao, J.; Zhang, T.; Dong, X.-Y.; Sun, M.-E.; Zhang, C.; Li, X.; Zhao, Y. S.; Zang, S.-Q. Circularly Polarized Luminescence from Achiral Single Crystals of Hybrid Manganese Halides. *Journal of the American Chemical Society* **2019**, *141* (40), 15755-15760.
- (8) Rajca, A.; Safronov, A.; Rajca, S.; Wongsriratanakul, J. D₂-Symmetric Dimer of 1,1'-Binaphthyl and Its Chiral Π -Conjugated Carbodianion. *Journal of the American Chemical Society* **2000**, *122* (14), 3351-3357.
- (9) Ananias, D.; Paz, F. A. A.; Yufit, D. S.; Carlos, L. D.; Rocha, J. Photoluminescent Thermometer Based on a Phase-Transition Lanthanide Silicate with Unusual Structural Disorder. *Journal of the American Chemical Society* **2015**, *137* (8), 3051-3058.
- (10) Vieru, V.; Ungur, L.; Chibotaru, L. F. Key Role of Frustration in Suppression of Magnetization Blocking in Single-Molecule Magnets. *The Journal of Physical Chemistry Letters* **2013**, *4* (21), 3565-3569.
- (11) Handzlik, G.; Magott, M.; Arczyński, M.; Sheveleva, A. M.; Tuna, F.; Sarewicz, M.; Osyczka, A.; Rams, M.; Vieru, V.; Chibotaru, L. F.; et al. Magnetization Dynamics and Coherent Spin Manipulation of a Propeller Gd(III) Complex with the Smallest Helicene Ligand. *The Journal of Physical Chemistry Letters* **2020**, *11* (4), 1508-1515.
- (12) Long, J.; Guari, Y.; Ferreira, R. A. S.; Carlos, L. D.; Larionova, J. Recent Advances in Luminescent Lanthanide Based Single-Molecule Magnets. *Coordination Chemistry Reviews* **2018**, *363*, 57-70.
- (13) Vonci, M.; Mason, K.; Sutura, E. A.; Frawley, A. T.; Worswick, S. G.; Kuprov, I.; Parker, D.; McInnes, E. J. L.; Chilton, N. F. Rationalization of Anomalous Pseudocontact Shifts and Their Solvent Dependence in a Series of C₃-Symmetric Lanthanide Complexes. *Journal of the American Chemical Society* **2017**, *139* (40), 14166-14172.
- (14) Görrler-Walrand, C.; Binnemans, K. Chapter 155 Rationalization of Crystal-Field Parametrization. *Handbook on the Physics and Chemistry of Rare Earths* **1996**, *23*, 121-283.
- (15) Chen, R.; Xu, Z.; Lin, Y.; Lv, B.; Bo, S.-H.; Zhu, H. Influence of Structural Distortion and Lattice Dynamics on Li-Ion Diffusion in Li₃OCl_{1-x}Br_x Superionic Conductors. *ACS Applied Energy Materials* **2021**, *4* (3), 2107-2114.
- (16) Liu, H.; Zhu, Z.; Yan, Q.; Yu, S.; He, X.; Chen, Y.; Zhang, R.; Ma, L.; Liu, T.; Li, M.; et al. A Disordered Rock Salt Anode for Fast-Charging Lithium-Ion Batteries. *Nature* **2020**, *585* (7823), 63-67.
- (17) Zabrodsky, H.; Peleg, S.; Avnir, D. Continuous Symmetry Measures. 2. Symmetry Groups and the Tetrahedron. *Journal of the American Chemical Society* **1993**, *115* (18), 8278-8289.
- (18) Dryzun, C.; Alemany, P.; Casanova, D.; Avnir, D. A Continuous Symmetry Analysis of Chemical Bonding. *Chemistry* **2011**, *17* (22), 6129-6141.

- (19) Alemany, P.; Casanova, D.; Dryzun, C. Electronic Structure and Symmetry in Conjugated Π -Electron Systems. *Chemistry – A European Journal* **2011**, *17* (52), 14896-14906.
- (20) Zabrodsky, H.; Peleg, S.; Avnir, D. Continuous Symmetry Measures. *Journal of the American Chemical Society* **1992**, *114* (20), 7843-7851.
- (21) Pinsky, M.; Avnir, D. Continuous Symmetry Measures. 5. The Classical Polyhedra. *Inorganic Chemistry* **1998**, *37* (21), 5575-5582.
- (22) Pinsky, M.; Dryzun, C.; Casanova, D.; Alemany, P.; Avnir, D. Analytical Methods for Calculating Continuous Symmetry Measures and the Chirality Measure. *Journal of Computational Chemistry* **2008**, *29* (16), 2712-2721.
- (23) Casanova, D.; Cirera, J.; Llunell, M.; Alemany, P.; Avnir, D.; Alvarez, S. Minimal Distortion Pathways in Polyhedral Rearrangements. *Journal of the American Chemical Society* **2004**, *126* (6), 1755-1763.
- (24) Alvarez, S.; Alemany, P.; Casanova, D.; Cirera, J.; Llunell, M.; Avnir, D. Shape Maps and Polyhedral Interconversion Paths in Transition Metal Chemistry. *Coordination Chemistry Reviews* **2005**, *249* (17), 1693-1708.
- (25) Ruiz-Martínez, A.; Alvarez, S. Stereochemistry of Compounds with Coordination Number Ten. *Chemistry – A European Journal* **2009**, *15* (30), 7470-7480.
- (26) Ruiz-Martínez, A.; Casanova, D.; Alvarez, S. Polyhedral Structures with an Odd Number of Vertices: Nine-Coordinate Metal Compounds. *Chemistry – A European Journal* **2008**, *14* (4), 1291-1303.
- (27) Zabrodsky, H.; Peleg, S.; Avnir, D. Symmetry as a Continuous Feature. *IEEE Transactions on pattern analysis and machine intelligence* **1995**, *17* (12), 1154-1166.
- (28) Zabrodsky, H.; Avnir, D. Continuous Symmetry Measures. 4. Chirality. *Journal of the American Chemical Society* **1995**, *117* (1), 462-473.
- (29) Llunell, M.; Casanova, D.; Cirera, J.; Alemany, P.; Alvarez, S. Shape, Version 2.1. *Universitat de Barcelona, Barcelona, Spain* **2013**, 2103.
- (30) Alvarez, S.; Alemany, P.; Casanova, D.; Cirera, J.; Llunell, M.; Avnir, D. Shape Maps and Polyhedral Interconversion Paths in Transition Metal Chemistry. *Coordination Chemistry Reviews* **2005**, *249* (17-18), 1693-1708.
- (31) Keinan, S.; Avnir, D. Continuous Symmetry Analysis of Tetrahedral/Planar Distortions. Copper Chlorides and Other $Ab(4)$ Species. *Inorganic Chemistry* **2001**, *40* (2), 318-323.
- (32) Pinsky, M.; Lipkowitz, K. B.; Avnir, D. Continuous Symmetry Measures. Vi. The Relations between Polyhedral Point-Group/Subgroup Symmetries. *Journal of Mathematical Chemistry* **2001**, *30* (1), 109-120.
- (33) Alvarez, S.; Avnir, D.; Llunell, M.; Pinsky, M. Continuous Symmetry Maps and Shape Classification. The Case of Six-Coordinated Metal Compounds. *New Journal of Chemistry* **2002**, *26* (8), 996-1009.
- (34) Alvarez, S.; Alemany, P.; Avnir, D. Continuous Chirality Measures in Transition Metal Chemistry. *Chemical Society Reviews* **2005**, *34* (4), 313-326.
- (35) Dryzun, C.; Avnir, D. Generalization of the Continuous Symmetry Measure: The Symmetry of Vectors, Matrices, Operators and Functions. *Physical Chemistry Chemical Physics* **2009**, *11* (42), 9653-9666.
- (36) Dryzun, C. Continuous Symmetry Measures for Complex Symmetry Group. *Journal of Computational Chemistry* **2014**, *35* (9), 748-755.
- (37) Alemany, P.; Casanova, D.; Alvarez, S.; Dryzun, C.; Avnir, D. Continuous Symmetry Measures: A New Tool in Quantum Chemistry. In *Reviews in Computational Chemistry, Vol 30*,

- Parrill, A. L., Lipkowitz, K. B. Eds.; Reviews in Computational Chemistry, Vol. 30; 2017; pp 289-352.
- (38) Thomsen, M. S.; Anker, A. S.; Kacenaikaite, L.; Sørensen, T. J. We Are Never Ever Getting (Back to) Ideal Symmetry: Structure and Luminescence in a Ten-Coordinated Europium(III) Sulfate Crystal *Submitted* **2022**.
- (39) Cirera, J.; Ruiz, E.; Alvarez, S. Stereochemistry and Spin State in Four-Coordinate Transition Metal Compounds. *Inorganic Chemistry* **2008**, *47* (7), 2871-2889.
- (40) Cirera, J.; Alemany, P.; Alvarez, S. Mapping the Stereochemistry and Symmetry of Tetracoordinate Transition-Metal Complexes. *Chemistry* **2004**, *10* (1), 190-207.
- (41) Alvarez, S.; Avnir, D.; Llunell, M.; Pinsky, M. Continuous Symmetry Maps and Shape Classification. The Case of Six-Coordinated Metal Compoundselectronic Supplementary Information (Esi) Available: Tables of Csd Refcodes, Structural Parameters and Symmetry Measures for the Studied Compounds. See <http://www.rsc.org/suppdata/nj/b2/b202096n>. *New Journal of Chemistry* **2002**, *26* (8), 996-1009.
- (42) Casanova, D.; Alemany, P.; Bofill, J. M.; Alvarez, S. Shape and Symmetry of Heptacoordinate Transition-Metal Complexes: Structural Trends. *Chemistry – A European Journal* **2003**, *9* (6), 1281-1295, <https://doi.org/10.1002/chem.200390145>.
- (43) Casanova, D.; Llunell, M.; Alemany, P.; Alvarez, S. The Rich Stereochemistry of Eight-Vertex Polyhedra: A Continuous Shape Measures Study. *Chemistry* **2005**, *11* (5), 1479-1494.
- (44) Ruiz-Martinez, A.; Casanova, D.; Alvarez, S. Polyhedral Structures with an Odd Number of Vertices: Nine-Atom Clusters and Supramolecular Architectures. *Dalton Trans* **2008**, (19), 2583-2591.
- (45) Ruiz-Martinez, A.; Casanova, D.; Alvarez, S. Polyhedral Structures with an Odd Number of Vertices: Nine-Coordinate Metal Compounds. *Chemistry* **2008**, *14* (4), 1291-1303.
- (46) Ruiz-Martinez, A.; Alvarez, S. Stereochemistry of Compounds with Coordination Number Ten. *Chemistry* **2009**, *15* (30), 7470-7480.
- (47) Carreras, A.; Bernuz, E.; Marugan, X.; Llunell, M.; Alemany, P. Effects of Temperature on the Shape and Symmetry of Molecules and Solids. *Chemistry – A European Journal* **2019**, *25* (3), 673-691, <https://doi.org/10.1002/chem.201801682>.
- (48) Tuvi-Arad, I.; Rozgonyi, T.; Stirling, A. Effect of Temperature and Substitution on Cope Rearrangement: A Symmetry Perspective. *The Journal of Physical Chemistry A* **2013**, *117* (48), 12726-12733.
- (49) Tuvi-Arad, I.; Stirling, A. The Distortive Nature of Temperature – a Symmetry Analysis. *Israel Journal of Chemistry* **2016**, *56* (11-12), 1067-1075, <https://doi.org/10.1002/ijch.201600045>.
- (50) Alvarez, S. Relationships between Temperature, Magnetic Moment, and Continuous Symmetry Measures in Spin Crossover Complexes. *Journal of the American Chemical Society* **2003**, *125* (22), 6795-6802.
- (51) Echeverría, J.; Alvarez, S. Application of Symmetry Operation Measures in Structural Inorganic Chemistry. *Inorganic Chemistry* **2008**, *47* (23), 10965-10970.
- (52) Ok, K. M.; Halasyamani, P. S.; Casanova, D.; Llunell, M.; Alemany, P.; Alvarez, S. Distortions in Octahedrally Coordinated D₀ Transition Metal Oxides: A Continuous Symmetry Measures Approach. *Chemistry of Materials* **2006**, *18* (14), 3176-3183.
- (53) Pilati, T.; Forni, A. Symmol: A Program to Find the Maximum Symmetry Group in an Atom Cluster, Given a Prefixed Tolerance. *Journal of Applied Crystallography* **1998**, *31* (3), 503-504, <https://doi.org/10.1107/S0021889898002180>.

- (54) Largent, R. J.; Polik, W. F.; Schmidt, J. R. Symmetrizer: Algorithmic Determination of Point Groups in Nearly Symmetric Molecules. *J Comput Chem* **2012**, *33* (19), 1637-1642.
- (55) Knowles, P. J. The Determination of Point Groups from Imprecise Molecular Geometries. *Journal of Mathematical Chemistry* **2021**, *60* (1), 161-171.
- (56) Alon, G.; Tuvi-Arad, I. Improved Algorithms for Symmetry Analysis: Structure Preserving Permutations. *Journal of Mathematical Chemistry* **2017**, *56* (1), 193-212.
- (57) Beruski, O.; Vidal, L. N. Algorithms for Computer Detection of Symmetry Elements in Molecular Systems. *J Comput Chem* **2014**, *35* (4), 290-299.
- (58) Pinsky, M.; Zait, A.; Bonjack, M.; Avnir, D. Continuous Symmetry Analyses: C(Nv) and D(N) Measures of Molecules, Complexes, and Proteins. *J Comput Chem* **2013**, *34* (1), 2-9.
- (59) Dryzun, C. Continuous Symmetry Measures for Complex Symmetry Group. *J Comput Chem* **2014**, *35* (9), 748-755.
- (60) Sheka, E. F.; Razbirin, B. S.; Nelson, D. K. Continuous Symmetry of C60 Fullerene and Its Derivatives. *The Journal of Physical Chemistry A* **2011**, *115* (15), 3480-3490.
- (61) Dryzun, C.; Avnir, D. Generalization of the Continuous Symmetry Measure: The Symmetry of Vectors, Matrices, Operators and Functions. *Phys Chem Chem Phys* **2009**, *11* (42), 9653-9666.
- (62) Casanova, D.; Alemany, P. Quantifying the Symmetry Content of the Electronic Structure of Molecules: Molecular Orbitals and the Wave Function. *Phys Chem Chem Phys* **2010**, *12* (47), 15523-15529.
- (63) Casanova, D.; Alemany, P.; Alvarez, S. Symmetry Measures of the Electron Density. *J Comput Chem* **2010**, *31* (13), 2389-2404.
- (64) Zhao, Y.; Truhlar, D. G. The M06 Suite of Density Functionals for Main Group Thermochemistry, Thermochemical Kinetics, Noncovalent Interactions, Excited States, and Transition Elements: Two New Functionals and Systematic Testing of Four M06-Class Functionals and 12 Other Functionals. *Theoretical Chemistry Accounts* **2008**, *120* (1), 215-241.
- (65) te Velde, G.; Bickelhaupt, F. M.; Baerends, E. J.; Fonseca Guerra, C.; van Gisbergen, S. J. A.; Snijders, J. G.; Ziegler, T. Chemistry with ADF. *Journal of Computational Chemistry* **2001**, *22* (9), 931-967.
- (66) Pye, C. C.; Ziegler, T. An Implementation of the Conductor-Like Screening Model of Solvation within the Amsterdam Density Functional Package. *Theoretical Chemistry Accounts* **1999**, *101* (6), 396-408.
- (67) Klamt, A.; Schuurmann, G. Cosmo: A New Approach to Dielectric Screening in Solvents with Explicit Expressions for the Screening Energy and Its Gradient. *Journal of the Chemical Society, Perkin Transactions 2* **1993**, (5), 799-805, 10.1039/P29930000799.
- (68) Shiery, R. C.; Fulton, J. L.; Balasubramanian, M.; Nguyen, M.-T.; Lu, J.-B.; Li, J.; Rousseau, R.; Glezakou, V.-A.; Cantu, D. C. Coordination Sphere of Lanthanide Aqua Ions Resolved with Ab Initio Molecular Dynamics and X-Ray Absorption Spectroscopy. *Inorganic Chemistry* **2021**, *60* (5), 3117-3130.
- (69) Storm Thomsen, M.; Anker, A. S.; Kacenauskaite, L.; Sørensen, T. J. We Are Never Ever Getting (Back to) Ideal Symmetry: Structure and Luminescence in a Ten-Coordinated Europium(III) Sulfate Crystal. *Dalton Transactions* **2022**, *51* (23), 8960-8963, 10.1039/D2DT01522F.
- (70) Dangelo, P.; Zitolo, A.; Migliorati, V.; Chillemi, G.; Duvail, M.; Vitorge, P.; Abadie, S.; Spezia, R. Revised Ionic Radii of Lanthanoid(III) Ions in Aqueous Solution. *Inorganic Chemistry* **2011**, *50* (10), 4572-4579.

- (71) R. Rüger, M. F., T. Trnka, A. Yakovlev, E. van Lenthe, P. Philipsen, T. van Vuren, B. Klumpers, T. Soini. S. Ams 2023.1, Theoretical Chemistry, Vrije Universiteit, Amsterdam, the Netherlands, [Http://Www.Scm.Com](http://www.scm.com). Contributors: R. Rüger, M. Franchini, T. Trnka, A. Yakovlev, E. Van Lenthe, P. Philipsen, T. Van Vuren, B. Klumpers, T. Soini.
- (72) Kabsch, W. A Solution for the Best Rotation to Relate Two Sets of Vectors. *Acta Crystallographica Section A* **1976**, 32 (5), 922-923.
- (73) Storm Thomsen, M.; Sørensen, T. J. Delicate, a Study of the Structural Changes in Ten-Coordinated La(Iii), Ce(Iii), Pr(Iii), Nd(Iii), Sm(Iii) and Eu(Iii) Sulfates. *Dalton Transactions* **2022**, 51 (23), 8964-8974, 10.1039/D2DT00832G.
- (74) Storm Thomsen, M.; Parsons, S.; Sørensen, T. J. Invisible Strings. The First Single Crystal of the Ctsap Form of [Eu(Dota)(H₂O)]⁻ Has an Electronic Structure Similar to One of the Reported Csap Forms. *Dalton Transactions* **2022**, 51 (41), 15725-15733, 10.1039/D2DT02633C.
- (75) Kuhn, H. W. The Hungarian Method for the Assignment Problem. *Naval Research Logistics Quarterly* **1955**, 2 (1-2), 83-97.
- (76) Nawrocki, P.; Sørensen, T. J. Optical Spectroscopy as a Tool for Studying the Solution Chemistry of Neodymium(Iii). *Physical Chemistry Chemical Physics* **2023**.
- (77) Persson, I.; D'Angelo, P.; De Panfilis, S.; Sandström, M.; Eriksson, L. Hydration of Lanthanoid(Iii) Ions in Aqueous Solution and Crystalline Hydrates Studied by Exafs Spectroscopy and Crystallography: The Myth of the "Gadolinium Break". *Chemistry – A European Journal* **2008**, 14 (10), 3056-3066, <https://doi.org/10.1002/chem.200701281>.
- (78) Thomson, J. J. Xxiv. On the Structure of the Atom: An Investigation of the Stability and Periods of Oscillation of a Number of Corpuscles Arranged at Equal Intervals around the Circumference of a Circle; with Application of the Results to the Theory of Atomic Structure. *The London, Edinburgh, and Dublin Philosophical Magazine and Journal of Science* **1904**, 7 (39), 237-265.
- (79) Drew, M. G. B. Structures of High Coordination Complexes. *Coordination Chemistry Reviews* **1977**, 24 (2-3), 179-275.
- (80) Hartshorn, R. M.; Hey-Hawkins, E.; Kalio, R.; Leigh, G. J. Representation of Configuration in Coordination Polyhedra and the Extension of Current Methodology to Coordination Numbers Greater Than Six (Iupac Technical Report). **2007**, 79 (10), 1779-1799.
- (81) Miniajluk, N.; Bondzior, B.; Stefańska, D.; Dereń, P. J. Eu³⁺ Ions in the Highly Symmetrical Octahedral Site in Ba₂MgWO₆ Double Perovskite. *Journal of Alloys and Compounds* **2019**, 802, 190-195.
- (82) Kang, J.-G.; 김택진. Luminescence and Crystal-Field Analysis of Europium and Terbium Complexes with Oxydiacetate and 1,10-Phenanthroline. *Bulletin of the Korean Chemical Society* **2005**, 26 (7), 1057-1064.
- (83) Pinto Marinho, E.; Araújo Melo, D. M.; Zinner, L. B.; Zinner, K.; Castellano, E. E.; Zukerman Schpector, J.; Isolani, P. C.; Vicentini, G. Neodymium(Iii) and Europium(Iii) Picrate Complexes with 2-Azacyclononane: Spectroscopy and Structure. *Polyhedron* **1997**, 16 (20), 3519-3523.
- (84) Nielsen, V. R. M.; Nawrocki, P. R.; Sørensen, T. J. Electronic Structure of Neodymium(Iii) and Europium(Iii) Resolved in Solution Using High-Resolution Optical Spectroscopy and Population Analysis. *The Journal of Physical Chemistry A* **2023**.
- (85) Kofod, N.; Nawrocki, P.; Sørensen, T. J. Arel: Investigating [Eu(H₂O)₉]³⁺ Photophysics and Creating a Method to Bypass Luminescence Quantum Yield Determinations. *The Journal of Physical Chemistry Letters* **2022**, 13 (13), 3096-3104.

- (86) Kofod, N.; Sørensen, T. J. Tb³⁺ Photophysics: Mapping Excited State Dynamics of [Tb(H₂O)₉]³⁺ Using Molecular Photophysics. *The Journal of Physical Chemistry Letters* **2022**, *13* (51), 11968-11973.
- (87) Thomsen, M. S.; Nawrocki, P. R.; Kofod, N.; Sørensen, T. J. Seven Europium(III) Complexes in Solution – the Importance of Reporting Data When Investigating Luminescence Spectra and Electronic Structure. *European Journal of Inorganic Chemistry* **2022**, *2022* (27), e202200334, <https://doi.org/10.1002/ejic.202200334>.
- (88) Binnemans, K. Interpretation of Europium(III) Spectra. *Coordination Chemistry Reviews* **2015**, *295*, 1-45.
- (89) Pinsky, M.; Casanova, D.; Alemany, P.; Alvarez, S.; Avnir, D.; Dryzun, C.; Kizner, Z.; Sterkin, A. Symmetry Operation Measures. *J Comput Chem* **2008**, *29* (2), 190-197.